

# Structure and stability of Al–Fe–Zr–Ce cluster: density functional study

Yifang Ouyang · Deming Zhai · Peng Wang ·  
Hongmei Chen · Yong Du · Yuehui He

Received: 8 January 2010 / Accepted: 16 May 2010 / Published online: 28 May 2010  
© Springer-Verlag 2010

**Abstract** The structure, stability and electronic properties of heteroatomic AB dimers, ABC trimers and ABCD tetramers ( $A, B, C, D = \text{Al}, \text{Fe}, \text{Zr}, \text{Ce}$ , and  $A \neq B \neq C \neq D$ ) have been systematically investigated by using a hybrid density functional B3LYP approach. All possible isomers for both trimers and tetramer are included in this work. The most stable geometry for trimers is found to be scalene triangle structure, and AlFeZrCe tetramer has a tetrahedral geometry as the ground state. The calculated spectroscopic constants are in good agreement with the available experimental and other theoretical results. The binding energy, HOMO-LUMO gap, excess charge, dipole moment and possible dissociation channels are also presented and discussed.

**Keywords** Cluster · Heteroatomic dimers, trimers and tetramer · Density functional theory · Electronic properties · Structure and stability

## 1 Introduction

The research field of cluster chemistry has exhibited a rapid development in both experiments and theory in the past two decades, because its has become of great interesting in many areas of science, such as material science, surface chemistry, chemical properties, thermal stability and

astrophysics. Clusters are on the border that separates molecules from liquids and solids [1, 2]. From atoms and molecules to liquids or solids, the evolution of structural and electronic properties of solid state is understood with the help of the studies of small clusters. Small clusters or nanoparticles exhibit properties that are often quite different from those in the bulk phase and change drastically with increasing cluster size. While a considerable amount of work has been conducted to study the structure and properties of unitary and binary clusters, no much attention has been paid to the study of properties of ternary and quaternary clusters. This is particularly surprising as dilute impurities are known to change the properties of bulk materials significantly. In small clusters, one or more dopant atoms amount to a large concentration change, and thus the properties of heteroatomic clusters are expected to be substantially influenced due to the presence of impurities. Therefore, determining geometrical and electronic properties of heteroatomic clusters is worthwhile.

Recently, the  $\text{Al}_n$  clusters containing from two to sixty atoms have been generated and characterized with different experimental techniques [3–8]. Experiments have been also performed in order to obtain the ionization potentials and the electron affinities for a large number of Al aggregates [3–8]. Previous theoretical literature on Al clusters is rich. The electronic structure of aluminum clusters has been studied systematically by ab initio theory [9–17]. The electronic structure of small aluminum clusters containing less than seven atoms is found to be consistent with aluminum being monovalent, while for larger clusters it behaves as a trivalent species. This behavior is rooted in the electronic structure of the aluminum atom itself. It has a  $3s^23p^1$  electronic configuration with an energy gap of approximately 5 eV separating the  $3s^2$  and  $3p^1$  shell. The physics of magnetic transition metal (TM) clusters is still

Y. Ouyang (✉) · D. Zhai · P. Wang · H. Chen  
Department of Physics, Guangxi University, Nanning 530004,  
People's Republic of China  
e-mail: ouyangyf@gxu.edu.cn

Y. Ouyang · Y. Du · Y. He  
State Key Laboratory of Powder Metallurgy, Central South  
University, Changsha 410083, People's Republic of China

an intriguing and challenging topic from both an experimental and a theoretical point of view. The electronic structure of small transition metal clusters (TMCs) has been studied with great interest. In particular, the properties of iron nanoclusters have been extensively investigated both in experiment [18–26] and in theory [27–38]. Investigations into  $\text{Fe}_n$  clusters reveal their strong size-dependent properties, which can be attributed to change in geometrical structures as number of atoms  $n$  increases. Zirconium atom, which is one of transition metal, has an electronic configuration of  $4d^25s^2$ . Zr is used in the nuclear industry for cladding fuel elements, because of its low absorption cross-section for neutrons and strong resistance to corrosion by many common acids, alkalis and sea water. Therefore, this metal, which is used as an alloying agent in steel and for making surgical appliances, is utilized extensively by the chemical industry where corrosive agents are employed. The resonant two-photo-ionization spectroscopy of  $\text{Zr}_2$  dimer [39] was investigated experimentally with laser ablation and jet-cooled molecular beam. Zhao et al. [40] and Wang et al. [41] measured the geometries and magnetisms of  $\text{Zr}_n$  ( $n = 2–16$ ) and  $\text{Zr}_n$  ( $n = 2–8$ ), respectively, using density functional theory. Additionally, lanthanide chemistry, which has been neglected for a long time, has undergone tremendous growth in recent years. It is now well known that the valence electronic structures of most lanthanide elements differ in their atomic forms from those of the corresponding bulk metal. The elemental Ce possesses a  $4f^15d^16s^2$  configuration. The vertical ionization potentials (VIPs) of  $\text{Ce}_2\text{–Ce}_{17}$  cluster were measured by photo-ionization mass spectrometry [42]. Recently, Cao et al. [43, 44] using CASSCF/MRCI method and Shen et al. [45] employing experiment have conducted further research on  $\text{Ce}_2$ . What is more, studies on bimetallic clusters have received great attention owing to their chemical and physical properties, which can be tuned by varying the composition, atomic ordering and size of the clusters [46]. Iron aluminides are an important class of intermetallic compounds with high oxidation and corrosion resistance, low density and interesting magnetic properties. According to the Al–Fe phase diagram, the bulk alloys form ordered  $\text{Fe}_3\text{Al}$  and  $\text{FeAl}$  compounds, which are ferromagnetic and non-magnetic, respectively. Recently, Reddy et al. [47] investigated the electronic structures and magnetism in  $(\text{FeAl})_n$  ( $n \leq 6$ ) clusters and found that the most stable structure of small clusters is dominated by a core of  $\text{Fe}_n$  atoms surrounded by the Al atoms. Ouyang et al. [48] have investigated the geometries, binding energy and multiplicity of  $\text{Al}_n\text{Fe}_m$  ( $n + m \leq 4$ ) using first-principles density functional calculations. Yin et al. [49] studied the electronic and magnetic properties of bimetallic  $\text{Fe}_m\text{Al}_n$  clusters with

$m + n < 5$  by BPW91/6-311++G(2d, 2p) method. Recently, Zhao et al. [50] determined the geometries and magnetism of  $\text{Zr}_n\text{Fe}$  ( $n = 2–13$ ) using ab initio calculations.

Motivated by the above discussion, in this article, we choose the aluminum, iron, zirconium and cerium atom, which constitute a potential bulk amorphous forming system, and investigated the evolution of heteroatomic cluster properties with the size of the system. The structure, stability and electronic properties of heteroatomic AB dimers, ABC trimers and ABCD tetramers (A, B, C, D = Al, Fe, Zr, Ce and A ≠ B ≠ C ≠ D) have been systematic investigated by density function theory. The calculated results are compared with the available experimental and other theoretical results.

## 2 Computational method

All the density functional calculations reported here implemented in the Gaussian 03 suite of programs [51]. As the experimental results for  $\text{Al}_2$ ,  $\text{Fe}_2$ ,  $\text{Zr}_2$  and  $\text{Ce}_2$  dimers are available [45, 52–57], we calculated the spectroscopic parameters (binding energies, bond distance and vibrational frequency) of these dimers using various exchange–correlation functionals. The exchange–correlation functionals we employed include BLYP, B3LYP, BP86, B3P86, BPW91, B3PW91, BPBE, PBEPBE, PBE1PBE and TPSS. Table 1 lists the calculated spectroscopic parameters of  $\text{Al}_2$ ,  $\text{Fe}_2$ ,  $\text{Zr}_2$  and  $\text{Ce}_2$  dimers together with experimental results. In Table 2, we also present the calculated total energies (a.u.) for  $\text{Fe}_2$  dimer and Fe monomer at each spin state with different DFT methods because of the large variation in binding energies from 1.10 to 4.39 eV. By comparing the present calculations with experimental results [45, 52–57], we find that the results obtained from B3LYP level are the closest to experimental data. Thus, we chose B3LYP in our calculation. In addition, we calculated the spin state of the lowest-energy structures for  $\text{Al}_2$ ,  $\text{Fe}_2$ ,  $\text{Zr}_2$  and  $\text{Ce}_2$  monomer with B3LYP method, the corresponding spin state is  ${}^3\Pi_u$ ,  ${}^9\Sigma_g^-$ ,  ${}^3\Delta_g$  and  ${}^3\Sigma_u^+$ , respectively. The B3LYP functional [58–60] is a combination of Becke's three-parameter hybrid exchange functional [59] and the Lee-Yang-Parr [59] correlation functional. Such an approach has proven to be a reliable tool studying of structure and stability.

The basis set used for Al is a standard Gaussian basis set 6-311++G (2d, 2p) that represents 6-311G set augmented with diffuse functions (++), two functions of type  $d$  on heavy atoms and two polarization functions of type  $p$  on hydrogen. As for transition metal Fe and Zr, the Lan12DZ

**Table 1** The calculated binding energy  $E_B$  (eV), bond distance  $R$  (Å) and vibrational frequency  $\omega_e$  ( $\text{cm}^{-1}$ ) for  $\text{Al}_2$ ,  $\text{Fe}_2$ ,  $\text{Zr}_2$  and  $\text{Ce}_2$  dimers with different DFT methods

| Method  | $\text{Al}_2$              |                             |                            | $\text{Fe}_2$     |                   |                            | $\text{Zr}_2$                |         |                            | $\text{Ce}_2$              |         |                            |
|---------|----------------------------|-----------------------------|----------------------------|-------------------|-------------------|----------------------------|------------------------------|---------|----------------------------|----------------------------|---------|----------------------------|
|         | $E_B$ (eV)                 | $R$ (Å)                     | $\omega_e(\text{cm}^{-1})$ | $E_B$ (eV)        | $R$ (Å)           | $\omega_e(\text{cm}^{-1})$ | $E_B$ (eV)                   | $R$ (Å) | $\omega_e(\text{cm}^{-1})$ | $E_B$ (eV)                 | $R$ (Å) | $\omega_e(\text{cm}^{-1})$ |
| BLYP    | 1.35                       | 2.797                       | 238.7                      | 1.88              | 2.043             | 399.1                      | 3.71                         | 2.357   | 311.4                      | 3.55                       | 2.616   | 242.4                      |
| B3LYP   | 1.33                       | 2.761                       | 256.0                      | 1.28              | 2.153             | 360.5                      | 3.01                         | 2.302   | 331.7                      | 3.08                       | 2.578   | 268.1                      |
| BP86    | 1.55                       | 2.500                       | 332.0                      | 1.99              | 2.026             | 410.1                      | 3.71                         | 2.317   | 312.9                      | 3.57                       | 2.585   | 266.2                      |
| B3P86   | 1.51                       | 2.734                       | 268.8                      | 1.19              | 2.137             | 368.3                      | 3.02                         | 2.281   | 335.5                      | 3.11                       | 2.551   | 290.2                      |
| BPW91   | 1.56                       | 2.495                       | 337.2                      | 3.25              | 2.031             | 405.6                      | 3.27                         | 2.317   | 307.9                      | 3.23                       | 2.595   | 276.9                      |
| B3PW91  | 1.48                       | 2.742                       | 267.4                      | 1.10              | 2.146             | 363.7                      | 2.65                         | 2.288   | 330.1                      | 2.79                       | 2.553   | 288.3                      |
| BPBE    | 1.57                       | 2.495                       | 338.1                      | 3.26              | 2.031             | 405.9                      | 3.27                         | 2.315   | 307.6                      | 3.25                       | 2.592   | 278.0                      |
| PBEPBE  | 1.65                       | 2.493                       | 340.0                      | 4.39              | 2.033             | 404.2                      | 3.63                         | 2.318   | 313.3                      | 3.54                       | 2.578   | 269.8                      |
| PBEIPBE | 1.52                       | 2.735                       | 272.2                      | 1.10              | 2.141             | 369.2                      | 2.61                         | 2.283   | 336.7                      | 2.83                       | 2.545   | 291.9                      |
| TPSS    | 1.51                       | 2.747                       | 262.2                      | 1.39              | 2.027             | 410.9                      | 3.37                         | 2.328   | 311.7                      | 2.96                       | 2.589   | 261.8                      |
| Expt.   | $1.34 \pm 0.06^{\text{a}}$ | $2.701 \pm 0.00^{\text{a}}$ | 284.2 <sup>b</sup>         | 1.30 <sup>c</sup> | 2.02 <sup>d</sup> | $300 \pm 15^{\text{e}}$    | $3.052 \pm 0.001^{\text{f}}$ | —       | —                          | $2.47 \pm 0.22^{\text{g}}$ | —       | $245.4 \pm 4.2^{\text{g}}$ |

The basis sets for Al, Fe, Zr and Ce are 6-311++G (2d, 2p), Lanl2DZ, Lanl2DZ and ECP46MWB, respectively

<sup>a</sup> See Ref. [52]

<sup>b</sup> See Ref. [53]

<sup>c</sup> See Ref. [54]

<sup>d</sup> See Ref. [55]

<sup>e</sup> See Ref. [56]

<sup>f</sup> See Ref. [57]

<sup>g</sup> See Ref. [45]

**Table 2** The calculated total energies (a.u.) for Fe<sub>2</sub> dimer and Fe monomer at each spin state with different DFT methods

| Method  | Fe <sub>2</sub> |              |              | Fe           |              |              |
|---------|-----------------|--------------|--------------|--------------|--------------|--------------|
|         | 1               | 3            | 5            | 7            | 9            | 1            |
| BLYP    | -246.6069596    | -246.6592962 | -246.6834424 | -246.7238105 | -246.7009062 | -123.1484437 |
| B3LYP   | -246.5919363    | -246.6267492 | -246.7078125 | -246.7589944 | -246.764676  | -123.2534284 |
| BP86    | -246.7716229    | -246.8871171 | -246.9117383 | -246.95094   | -246.9289787 | -123.292463  |
| B3P86   | -247.3023664    | -247.3401798 | -247.4235233 | -247.4735289 | -247.478479  | -123.5936894 |
| BPW91   | -246.7916061    | -246.8525263 | -246.8972187 | -246.938403  | -246.9194562 | -123.2632044 |
| B3PW91  | -246.6348072    | -246.6735128 | -246.7602837 | -246.8124677 | -246.8218402 | -123.2659378 |
| BPBE    | -246.7065496    | -246.8045806 | -246.8495093 | -246.8909309 | -246.8724371 | -122.9913393 |
| PBEPBE  | -246.5303398    | -246.7168793 | -246.743497  | -246.78704   | -246.7684267 | -123.1378804 |
| PBEIPBE | -246.420229     | -246.4711087 | -246.570561  | -246.6261191 | -246.6440334 | -123.17245   |
| TPSS    | -246.503541     | -246.5847408 | -246.6380359 | -246.6776788 | -246.6696791 | -123.0722142 |

The basis sets for Fe are Lanl2DZ

basis set [61] of double- $\zeta$  quality was employed. The effective core potentials are used, and mass-velocity and Darwin relativistic effects are incorporated in Lanl2DZ. For Ce atom, we choose the small core relativistic effective core potential (RECP) developed by Huelsen et al. [62] namely, ECP46MWB, and both the RECP and basis sets for Ce can be found at the Web site of Stuttgart group [63].

In our calculations, to avoid trapping at local minima of the potential energy surface, different initial geometry of heteroatomic AB dimers, ABC trimers and ABCD tetramers (A, B, C, D = Al, Fe, Zr, Ce and A ≠ B ≠ C ≠ D) are considered. The stability of optimized geometries was reassured accurately by computing the harmonic vibrational frequency calculation (no negative frequency). In addition, for each isomer, various possible spin multiplicities are considered until the total energy increases with increasing S. The calculated binding energy per atom for the most stable cluster is defined as

$$E_B = \frac{E(A) + E(B) - E(AB)}{2} \quad (1)$$

$$E_B = \frac{E(A) + E(B) + E(C) - E(ABC)}{3} \quad (2)$$

$$E_B = \frac{E(A) + E(B) + E(C) + E(D) - E(ABCD)}{4} \quad (3)$$

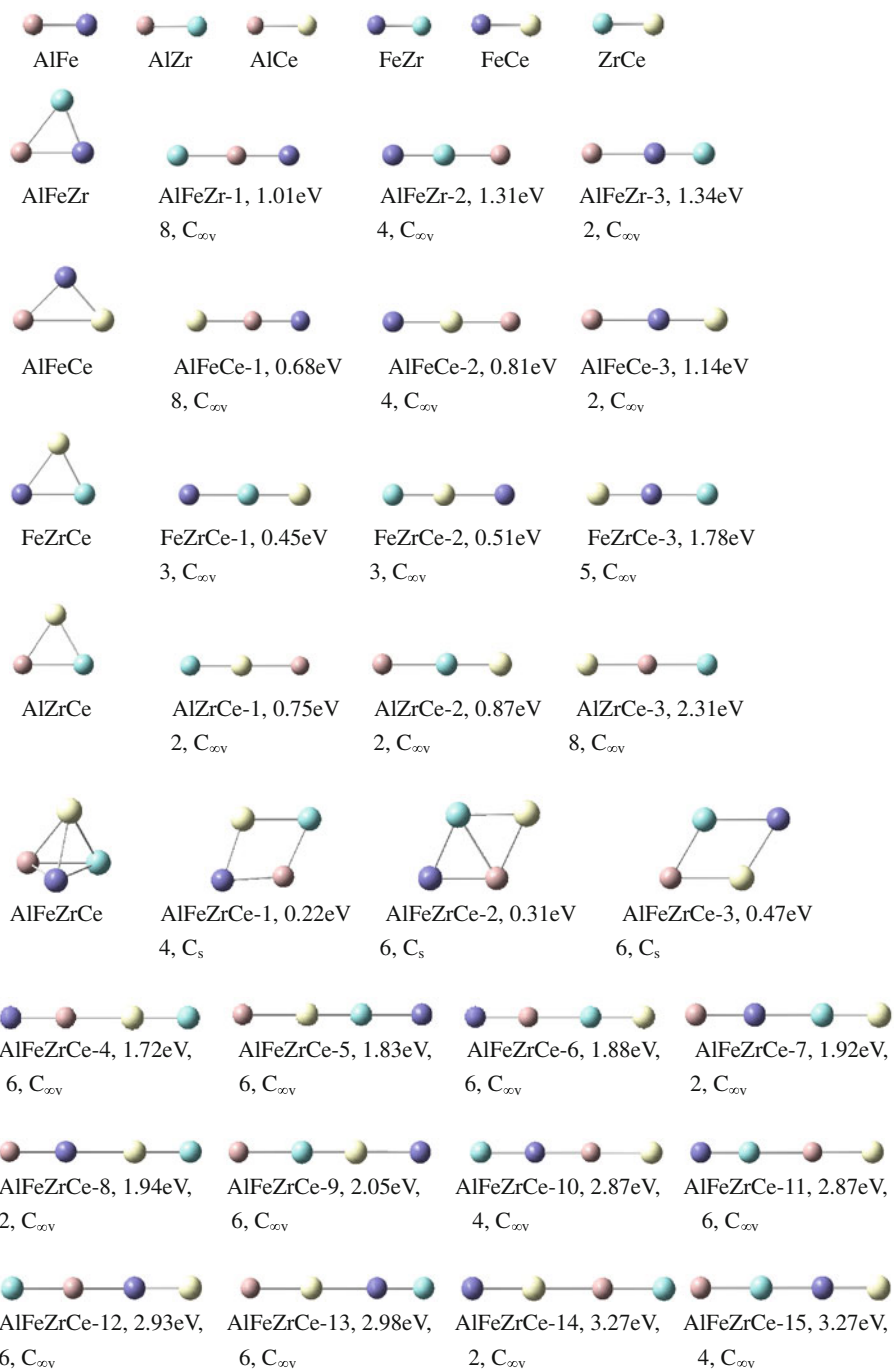
where  $E(A)$ ,  $E(B)$ ,  $E(C)$  and  $E(D)$  are the energies of the isolated atoms A, B, C and D, respectively, and  $E(AB)$ ,  $E(ABC)$  and  $E(ABCD)$  represent the energies of the corresponding stable geometry of AB dimers, ABC trimers and ABCD tetramer, respectively.

### 3 Results and discussions

#### 3.1 Geometry optimization

We have searched for possible isomers on heteroatomic AB dimers, ABC trimers and ABCD tetramer (A, B, C, D = Al, Fe, Zr, Ce and A ≠ B ≠ C ≠ D), as shown in Fig. 1, according to their composition, the number of atoms, spin multiplicity, symmetry and relative energy. Table 3 presents the ground state symmetry, state, spin multiplicity, bond length, as well as harmonic vibrational frequencies for AB, ABC and ABCD clusters. Our calculated binding energy and the energy gap between the highest occupied molecular orbital (HOMO) and the lowest unoccupied molecular orbital (LUMO) are listed in Table 4. The calculated excess charge (in units of electron charge) on atoms and dipole moment (in Debye) are shown in Table 5. We also calculated the possible dissociation channels and the corresponding dissociation energies, which are presented in Table 6. To assess the accuracy of our calculations, some available experimental and

**Fig. 1** Low-energy isomers for Al–Fe–Zr–Ce clusters at the B3LYP level; red, blue, green and yellow color balls represent aluminum, iron, zirconium and cerium atoms, respectively. The texts under the structure are relative energies (in eV) with respect to those of the corresponding lowest-energy isomers, spin multiplicity and symmetry, respectively



theoretical values for the considered clusters are also included in Table 3.

### 3.1.1 Dimers

For these six dimers (AlFe, AlZr, AlCe, FeZr, FeCe and ZrCe), no experimental studies are available for them. Our investigations indicate that the ground state of AlFe is at spin multiplicity 4 ( ${}^4\Sigma^{-1}$ ) with bond length 2.4544 Å and vibrational frequency 283.2 cm<sup>-1</sup>, which are in excellent

agreement with values of 2.4538 Å and 285.9 cm<sup>-1</sup> reported by Ouyang et al. [64]. Compared with other calculations (2.41 and 2.42 Å) performed by Reddy et al. [47] and Yin et al. [49], respectively, our calculated bond length is slightly overestimate. The results (2.50 Å, 280.1 cm<sup>-1</sup>) obtained by previous studies [48] are also reasonable consistent with our results. For AlZr dimer, the calculated spectroscopic constants ( $\Delta^6$ , 2.6506 Å, 291.7 cm<sup>-1</sup>) are in excellent agreement with the available theoretical values [64] ( $\Delta^6$ , 2.6505 Å, 291.4 cm<sup>-1</sup>). Among the six dimers,

**Table 3** Symmetries, state, spin multiplicity, bond length (in Å) and harmonic vibrational frequencies (in cm<sup>-1</sup>) of the lowest-energy structures of Al–Fe–Zr–Ce clusters

| Str.     | Sym.           | Sta.         | S | $R_{\text{Al-Fe}}$ | $R_{\text{Al-Zr}}$ | $R_{\text{Al-Ce}}$ | $R_{\text{Fe-Zr}}$ | $R_{\text{Fe-Ce}}$ | $R_{\text{Zr-Ce}}$ | Frequencies                              |
|----------|----------------|--------------|---|--------------------|--------------------|--------------------|--------------------|--------------------|--------------------|--|
| AlFe     | $C_{\infty v}$ | $^4\Sigma^-$ | 4 | 2.4544             |                    |                    |                    |                    |                    | 283.2                                    |
| AlZr     | $C_{\infty v}$ | $\Delta^6$   | 6 |                    | 2.6506             |                    |                    |                    |                    | 291.7                                    |
| AlCe     | $C_{\infty v}$ | $\Delta^6$   | 6 |                    |                    | 2.8271             |                    |                    |                    | 258.8                                    |
| FeZr     | $C_{\infty v}$ | $\Delta^3$   | 3 |                    |                    |                    | 2.3969             |                    |                    | 180.7                                    |
| FeCe     | $C_{\infty v}$ | $\Delta^3$   | 3 |                    |                    |                    |                    | 2.4120             |                    | 186.4                                    |
| ZrCe     | $C_{\infty v}$ | $\Delta^3$   | 3 |                    |                    |                    |                    |                    | 2.4589             | 274.5                                    |
| AlFeZr   | $C_s$          | $^2A'$       | 2 | 2.6068             | 2.7697             |                    | 2.3444             |                    |                    | 158.0, 175.5, 259.9                      |
| AlFeCe   | $C_s$          | $^2A''$      | 2 | 2.5620             |                    | 2.7958             |                    | 2.5546             |                    | 169.7, 177.5, 271.7                      |
| FeZrCe   | $C_s$          | $^3A''$      | 3 |                    |                    |                    | 2.8988             | 2.7836             | 2.5599             | 107.4, 140.7, 266.8                      |
| AlZrCe   | $C_s$          | $^4A''$      | 4 |                    | 2.8596             | 2.8460             |                    |                    | 2.6299             | 150.0, 180.4, 269.4                      |
| AlFeZrCe | $C_1$          | $^6A$        | 6 | 2.5791             | 2.7670             | 2.9697             | 2.7759             | 2.8261             | 2.6709             | 107.7, 122.4, 155.1, 183.1, 190.9, 275.3 |

Ref. [64] 2.4538 Å, 285.9 cm<sup>-1</sup>; 2.6505 Å, 291.4 cm<sup>-1</sup>, Ref. [47] 2.41 Å, Ref. [49] 2.42 Å, Ref. [48] 2.50 Å, 280.1 cm<sup>-1</sup>

**Table 4** Calculated binding energy (in eV/atom), HOMO, LUMO energies (in Hartrees) and HOMO-LUMO gap ( $E_g$ ) energies (in eV) of the lowest-energy structures of Al–Fe–Zr–Ce clusters

| Clusters | $E_B/\text{atom}$ | HOMO( $\alpha$ ) | LUMO( $\alpha$ ) | $E_g(\alpha)$ | HOMO( $\beta$ ) | LUMO( $\beta$ ) | $E_g(\beta)$ |
|----------|-------------------|------------------|------------------|---------------|-----------------|-----------------|--------------|
| AlFe     | 1.0892            | -0.1794          | -0.0761          | -2.8109       | -0.1709         | -0.0744         | -2.6273      |
| AlZr     | 0.8660            | -0.1534          | -0.0618          | -2.4907       | -0.2814         | -0.0937         | -5.1073      |
| AlCe     | 0.9086            | -0.1479          | -0.0766          | -1.9396       | -0.2837         | -0.0839         | -5.4377      |
| FeZr     | 1.0882            | -0.1424          | -0.0694          | -1.9875       | -0.1705         | -0.0849         | -2.3290      |
| FeCe     | 0.9330            | -0.1287          | -0.0790          | -1.3549       | -0.1551         | -0.0724         | -2.2512      |
| ZrCe     | 1.5379            | -0.1369          | -0.0759          | -1.6599       | -0.1497         | -0.0746         | -2.0436      |
| AlFeZr   | 1.5234            | -0.1626          | -0.0781          | -2.2986       | -0.1767         | -0.0982         | -2.1366      |
| AlFeCe   | 1.4169            | -0.1462          | -0.0940          | -1.4221       | -0.1534         | -0.0887         | -1.7609      |
| FeZrCe   | 1.7436            | -0.1316          | -0.0769          | -1.4887       | -0.1393         | -0.0794         | -1.6297      |
| AlZrCe   | 1.7077            | -0.1550          | -0.0981          | -1.5478       | -0.1562         | -0.0936         | -1.7043      |
| AlFeZrCe | 1.9527            | -0.1530          | -0.0981          | -1.4931       | -0.1549         | -0.0935         | -1.6702      |

**Table 5** Calculated excess charge (in units of electron charge) on atoms and dipole moments (in Debye) of Al–Fe–Zr–Ce clusters

| Clusters | $q(\text{Al})$ | $q(\text{Fe})$ | $q(\text{Zr})$ | $q(\text{Ce})$ | $\mu_x$ | $\mu_y$ | $\mu_z$ | $\mu$  |
|----------|----------------|----------------|----------------|----------------|---------|---------|---------|--------|
| AlFe     | 0.1318         | -0.1318        |                |                | 0.0000  | 0.0000  | 0.3499  | 0.3499 |
| AlZr     | -0.0077        |                | 0.0077         |                | 0.0000  | 0.0000  | 2.2574  | 2.2574 |
| AlCe     | 0.0752         |                |                | -0.0752        | 0.0000  | 0.0000  | 1.9056  | 1.9056 |
| FeZr     |                | 0.0499         | -0.0499        |                | 0.0000  | 0.0000  | 0.7747  | 0.7747 |
| FeCe     |                | -0.2144        |                | 0.2144         | 0.0000  | 0.0000  | 3.0736  | 3.0736 |
| ZrCe     |                |                | -0.1975        | 0.1975         | 0.0000  | 0.0000  | 1.5433  | 1.5433 |
| AlFeZr   | 0.0312         | -0.2383        | 0.2072         |                | -1.0974 | 2.5395  | 0.0000  | 2.7664 |
| AlFeCe   | 0.0391         | -0.2232        |                | 0.1841         | -1.2101 | 3.3495  | 0.0000  | 3.5614 |
| FeZrCe   |                | -0.1308        | -0.1483        | 0.2791         | 0.2175  | 2.0217  | 0.0000  | 2.0334 |
| AlZrCe   | -0.0027        |                | -0.0992        | 0.1019         | -1.8298 | 1.9262  | 0.0000  | 2.6568 |
| AlFeZrCe | 0.0401         | -0.2969        | -0.0201        | 0.2769         | -1.7241 | -1.6233 | -1.7760 | 2.9600 |

as can be seen in Table 3, the present calculated values for bond length are all in range of 2.3969–2.8271 Å. It is notable that the bond length of FeZr is the shortest, and the

corresponding vibrational frequency is the lowest. It is interesting that the ground state of AB (A, B = Fe, Zr, Ce, A ≠ B) is at spin multiplicity of 3 ( $\Delta^3$ ), and the bond

**Table 6** Dissociation data of the lowest-energy structures of Al–Fe–Zr–Ce clusters: the possible dissociation channels and corresponding dissociation energies are in eV

| Clusters |          | Dissociation channel      | Dissociation energy |
|----------|----------|---------------------------|---------------------|
| AlFe     | AlFe     | $\rightarrow$ Al + Fe     | −2.1784             |
| AlZr     | AlZr     | $\rightarrow$ Al + Zr     | −1.7320             |
| AlCe     | AlCe     | $\rightarrow$ Al + Ce     | −1.8171             |
| FeZr     | FeZr     | $\rightarrow$ Fe + Zr     | −2.1763             |
| FeCe     | FeCe     | $\rightarrow$ Fe + Ce     | −1.8660             |
| ZrCe     | ZrCe     | $\rightarrow$ Zr + Ce     | −3.0758             |
| AlFeZr   | AlFeZr   | $\rightarrow$ AlFe + Zr   | −2.3919*            |
|          |          | FeZr + Al                 | −2.3939             |
|          |          | AlZr + Fe                 | −2.8385             |
|          |          | Al + Fe + Zr              | −4.5703             |
| AlFeCe   | AlFeCe   | $\rightarrow$ AlFe + Ce   | −2.0724*            |
|          |          | FeCe + Al                 | −2.3847             |
|          |          | AlCe + Fe                 | −2.4337             |
|          |          | Al + Fe + Ce              | −4.2508             |
| FeZrCe   | FeZrCe   | $\rightarrow$ ZrCe + Fe   | −2.1549*            |
|          |          | FeZr + Ce                 | −3.0544             |
|          |          | FeCe + Zr                 | −3.3647             |
|          |          | Fe + Zr + Ce              | −5.2307             |
| AlZrCe   | AlZrCe   | $\rightarrow$ ZrCe + Al   | −2.0472*            |
|          |          | AlCe + Zr                 | −3.3059             |
|          |          | AlZr + Ce                 | −3.3910             |
|          |          | Al + Zr + Ce              | −5.1230             |
| AlFeZrCe | AlFeZrCe | $\rightarrow$ AlFe + ZrCe | −2.5565*            |
|          |          | FeZrCe + Al               | −2.5801             |
|          |          | AlZrCe + Fe               | −2.6878             |
|          |          | AlFeZr + Ce               | −3.2405             |
|          |          | AlFeCe + Zr               | −3.5600             |
|          |          | AlCe + FeZr               | −3.8173             |
|          |          | AlZr + FeCe               | −4.2128             |
|          |          | ZrCe + Al + Fe            | −4.7349             |
|          |          | AlFe + Zr + Ce            | −5.6324             |
|          |          | FeZr + Al + Ce            | −5.6345             |
|          |          | FeCe + Al + Zr            | −5.9448             |
|          |          | AlCe + Fe + Zr            | −5.9937             |
|          |          | AlZr + Fe + Ce            | −6.0788             |
|          |          | Al + Fe + Zr + Ce         | −7.8108             |

The asterisked rows represent the favorable dissociation for the corresponding clusters

distance of FeX ( $X = \text{Al}, \text{Zr}, \text{Ce}$ ) is smaller than the other AB ( $A \neq B$ ) dimers consisting of Al, Zr and Ce atom. For the homoatomic dimers, as shown in Table 1, the bond distances (2.153, 2.302 Å) of  $\text{Fe}_2$  and  $\text{Zr}_2$  dimers are shorter than others ( $\text{Al}_2$ :2.761,  $\text{Ce}_2$ :2.578 Å), that may be the reason why the FeZr dimer has the shortest bond length in all binary dimers. We also find that the bond distances of

$\text{FeX}$  ( $X = \text{Al}, \text{Zr}, \text{Ce}$ ) and  $\text{ZrX}$  ( $X = \text{Al}, \text{Fe}, \text{Ce}$ ) heteroatomic dimers are longer than the corresponding  $\text{Fe}_2$  and  $\text{Zr}_2$  homoatomic dimers; however, the bond distance of  $\text{AlX}$  and  $\text{CeX}$  ( $X = \text{Fe}, \text{Zr}$ ) dimers is smaller than  $\text{Al}_2$  and  $\text{Ce}_2$  dimers. The above discussion may be result from the A and B atoms which possess different electronic configuration.

### 3.1.2 Trimmers

For these species, as well as the heteroatomic dimers discussed above, all the calculated results (bond lengths and vibrational frequencies) are given in Table 3. We have not found experimental data for these heteronuclear species in literature. Data for these clusters were indeed quite limited. Our investigations indicate that the lowest-energy geometry of AlFeZr, AlFeCe, AlZrCe and FeZrCe heteroatomic trimers is the scalene triangle with  $C_s$  symmetry. Additionally, we also tried the linear geometry. However, the energies of them are higher than those of triangle structures. There are three possible isomer structures for each trimer. Take AlFeZr trimer for example, the linear geometry with  $C_{\infty v}$  asymmetry has three isomer structures: Al–Fe–Zr, Fe–Zr–Al and Zr–Al–Fe. Figure 1 shows that Al atom occupying a central position is lower by 0.30 or 0.33 eV than that of Zr or Fe atom taking a central position, respectively. We also find that there is a similar tendency for another AlFe-contained cluster (AlFeCe), and the corresponding spin multiplicity and stability for linear structures are the same as those of AlFeZr. From Fig. 1, it is concluded that the linear Fe-containing species (A–Fe–C), in which Fe atom occupying a central position, have the worst stability compared with the other structures. Furthermore, the calculated values from the present work indicate that the bond lengths (A–B, B–C and A–C) of ZrCe-containing trimers are longer than those of dimers.

### 3.1.3 Tetramer

There are a large number of possible isomers for AlFeZrCe tetramer, and the initial trial geometries considered for the tetramer are tetrahedron, rhombus and line structures. The corresponding various structures are presented in Fig. 1. We also tried the Y-planar structure, but it was found that this structure is not stable. Our calculated results indicate that AlFeZrCe tetramer has three-dimensional geometry ( $C_1$ ) as the energetically most favorable with the spin multiplicity of six. The corresponding spectroscopic constants of the energetically preferred state are given in Table 3, and our result for vibration is  $275.3 \text{ cm}^{-1}$  as the maximum amplitude. It can be observed from Fig. 1 that the planar structures (AlFeZrCe-1, AlFeZrCe-2 and AlFeZrCe-3) with  $C_s$  symmetry are more stable than the linear

isomers. Those planar structures are only higher by 0.22, 0.31 and 0.47 eV than the ground-state structure ( $\text{Al}-\text{FeZrCe}$ ), respectively. We also find that the  $\text{Al}-\text{Zr}-\text{Fe}-\text{Ce}$  linear structure of tetramer ( $\text{AlFeZrCe-15}$ ) has the worst stability due to the highest relative energy (3.27 eV) compared with the ground state of tetramer, i.e. tetrahedron. Furthermore, the bond lengths ( $\text{Al-Fe}$ ,  $\text{Al-Zr}$ ,  $\text{Al-Ce}$ ,  $\text{Fe-Zr}$ ,  $\text{Fe-Ce}$  and  $\text{Zr-Ce}$ ) for  $\text{AlFeZrCe}$  tetramer are systematically more elongated compared with those of corresponding dimers, which may be explained by the significant change in the geometry of cluster.

### 3.2 Energetics of clusters

The binding energy, the HOMO, the LUMO and HOMO-LUMO gap of the heteroatomic clusters considered are computed in this work, which are given in Table 4. It can be seen that the binding energies ( $E_B$  in eV/atom) of  $\text{ZrCe}$  dimer and  $\text{FeZrCe}$  trimer are larger than those of the other dimers and trimers, respectively. Furthermore, we notice that the binding energy  $E_B$  (1.9527 eV) of  $\text{AlFeZrCe}$  tetramer is the biggest among all the clusters, and the increasing binding energy indicates that the formation of clusters is favorable process. The position of HOMO, LUMO and the HOMO-LUMO gap bear important from a spectroscopic point of view. The most striking feature is that the calculated HOMO-LUMO energy gaps of dimers are relatively bigger than those of the trimers and tetramer. Another feature is that the gaps of  $\alpha$  states are relatively smaller than those of  $\beta$  states, except  $\text{AlFe}$  and  $\text{AlFeZr}$  clusters.

The calculated excess charge and dipole moments of clusters are given in Table 5. Because of their special symmetry, all the clusters experience charge separations among the atoms, resulting in non-zero dipole moments. The charge transfer between the constituents of a compound is determined by the electronegative of constituents. The bigger electronegative is, the stronger electron attraction is, so the atom usually gets more valence electrons. The electronegatives of Al, Fe, Zr and Ce are 1.61, 1.83, 1.33 and 1.12, respectively. According to natural population analysis, for Al-containing dimers, it is can be seen from Table 5 that the charge transfers from Al to Fe and Ce atom, respectively, and Al gets charge 0.0077e from Zr atom. The present calculations indicate that  $\text{AlFe}$  and  $\text{AlZr}$  dimers are agreement with the above rule. However, Ce is negative ( $-0.0752e$ ) for  $\text{AlCe}$ , this may be the reason for the special electronic structure ( $4f^15d^16s^2$ ) of Ce atom. For AlFe-containing trimers, Fe atom gets charge total 0.2383e (0.2232e) from Al and Zr (Ce) atoms, respectively, because of the bigger electronegative compared with Al, Zr and Ce atom. We also found that the charge transfers from Ce to the other two atoms (Fe and Zr, Al and Zr) for the  $\text{ZrCe}$

containing trimers due to the smallest electronegative among them. For  $\text{AlFeZrCe}$  tetramer, the charge on Al is more negative than that on Zr atom. The calculated values indicate that Fe and Zr atoms get total 0.3170e from Al and Ce atoms. We note that all the clusters bear a net dipole moment, as expected, ranging from 0.3499 to 3.5614 Debye.

### 3.3 Cluster stability

To give more insight into the stability of the  $\text{Al-Fe-Zr-Ce}$  heteroatomic microcluster, we could investigate the dissociation process of cluster. In the present work, we considered all possible dissociation channels. The possible dissociation channels and the corresponding dissociation energy are presented in Table 6. All the dissociation energies are negative, as should be. In all the case, the energetically lowest fragmentation channel corresponds to the loss of a single atom, except for  $\text{AlFeZrCe}$  tetramer. Our investigations indicate that  $\text{AlFeZrCe}$  cluster prefers to break into  $\text{AlFe}$  and  $\text{ZrCe}$  dimers. There are four dissociation channels for each trimer. Table 6 clearly indicates that AlFe-containing and ZrCe-containing trimers favor dissociation via the channel AlFe (ZrCe)-containing trimer  $\rightarrow$  AlFe (ZrCe) + C, consistent with the fact that AlFe and ZrCe have a large binding energy (1.0892 and 1.5379 eV, respectively) among the dimers. This may be the reason why  $\text{AlFeZrCe}$  tetramer would like to break into AlFe and ZrCe dimers instead of to the loss of a single atom.

## 4 Conclusions

The equilibrium structure, energetics and stabilities of heteroatomic AB dimers, ABC trimers and ABCD tetramer ( $A, B, C, D = \text{Al}, \text{Fe}, \text{Zr}, \text{Ce}$  and  $A \neq B \neq C \neq D$ ) have been studied using a hybrid density functional method B3LYP. According to the present investigations, the most stable structure of ABC trimers is found to be scalene triangle structure, and  $\text{AlFeZrCe}$  tetramer has a tetrahedral geometry as ground state. The calculated spectroscopic constants are in good agreement with the available experimental and the other theoretical results. It can be seen that the binding energies of  $\text{ZrCe}$  dimer and  $\text{FeZrCe}$  trimer are larger than those of the other dimers and trimers, and the binding energy (1.9527 eV) of  $\text{AlFeZrCe}$  tetramer is the biggest among all the clusters. The HOMO-LUMO energy gaps of  $\alpha$  states are relatively smaller than those of  $\beta$  states, except  $\text{AlFe}$  and  $\text{AlFeZr}$  clusters. The excess charge and dipole moment of clusters are also presented and discussed. It can be seen that the above results are reasonable, which are access to the properties of the bulks. The results of the

dissociation energies indicate that the clusters are priority to the loss of a single atom except AlFeZrCe species which prefers to break into AlFe and ZrCe dimers, and AlFe (ZrCe)-bearing trimers favor to fragment consist of AlFe (ZrCe) dimer first.

**Acknowledgments** This work was financially supported by the National Natural Science Foundation of China (50761002 and 50831007) and Guangxi Natural Science Foundation (0832007). This work was also partly supported by State Key Laboratory of Powder Metallurgy, Central South University, China.

## References

1. Haberland H (ed) (1994) Clusters of atoms and molecules, Springer, Berlin
2. Haberland H (ed) (1994) Clusters of atoms and molecules II, Springer, New York
3. Cox DM, Trevor DJ, Whetten L, Rohfling EA, Kaldor A (1986) *J Chem Phys* 84:4651
4. Hanley L, Anderson SL (1986) *Chem Phys Lett* 129:429
5. Jarrold MF, Bower JE, Kraus JS (1987) *J Chem Phys* 86:3876
6. Gantefor G, Gausa M, Meiweis-Broer KH, Lutze HO (1988) *Z. Phys. D* 9:253
7. Taylor KJ, Pettiette CL, Craycraft MJ, Chesnovsky O, Smatley RE (1988) *Chem Phys Lett* 152:347
8. Schriver KE, Persson JL, Honea EC, Whetten RL (1990) *Phys Rev Lett* 64:2539
9. Rao BK, Jena P (1999) *J Chem Phys* 111:1890
10. Gong XG, Kumar V (1993) *Phys Rev Lett* 70:2078
11. Ahlrichs R, Elliott SD (1999) *Phys. Chem. Chem. Phys.* 1:13
12. Akola J, Hakkinen H, Manninen M (1998) *Phys. Rev. B* 58:3601
13. Petterson LGM, Bauschlicher CW Jr, Halicioglu T (1987) *J Chem Phys* 87:2205
14. Ray AK, Rao BK (1997) *J. Phys.: Condens. Matter* 9:2859
15. Deshpande MD, Kanhere DG, Vasiliev I, Martin RM (2003) *Phys. Rev. B* 68:035428
16. Calaminici P, Russo N, Toscano M (1995) *Z. Phys. D* 33:281
17. Li GF, Peng P, Qiu ZQ, Yang F, Han SC (2006) *Chin J Non-ferrous Met* 16:0823
18. Parks EK, Weiller BH, Bechtold PS, Hoffman WF, Nieman GC, Pobo LG, Riley SJ (1998) *J Chem Phys* 88:1622
19. Liyanage R, Griffin JB, Armentrout PB (2003) *J Chem Phys* 119:8979
20. Pellarin M, Baguenard B, Vialle JL, Lerme J, Broyer M, Miller J, Perez A (1994) *Chem Phys Lett* 217:349
21. Lian L, Su CX, Armentrout PB (1992) *J Chem Phys* 97:4072
22. de Heer WA, Milani P, Chatelain A (1990) *Phys Rev Lett* 65:488
23. Billas IML, Becker JA, Chatelain A, de Heer WA (1993) *Phys Rev Lett* 71:4067
24. Billas IML, Chatelain A, de Heer WA (1994) *Science* 265:1682
25. Wang LS, Cheng HS, Fan J (1995) *J Chem Phys* 102:9480
26. Sakurai M, Watanabe K, Sumiyama K, Suzuki K (1999) *J Chem Phys* 111:235
27. Chen JL, Wang CS, Jackson KA, Pederson MR (1991) *Phys Rev B* 44:6558
28. Castro M, Salahub DR (1994) *Phys Rev B* 49:11842
29. Ballone P, Jones RO (1995) *Chem Phys Lett* 233:632
30. Oda T, Pasquarello A, Car R (1998) *Phys Rev Lett* 80:3622
31. Dieguez O, Alemany MMG, Rey C, Ordejon P, Gallego LJ (2001) *Phys Rev B* 63:205407
32. Andriotis AN, Menon M (1998) *Phys Rev B* 57:10069
33. Franco JA, Vega A, Aguilera-Granja F (1999) *Phys Rev B* 60:434
34. Boyukata M, Borges E, Braga JP, Belchior JC (2005) *J Alloys Compd* 403:349
35. Kohler C, Seifert G, Frauenheim T (2005) *Chem Phys* 309:23
36. Rollmann G, Entel P, Sahoo S (2006) *Comput Mater Sci* 35:275
37. Ma QM, Xie Z, Wang J, Liu Y, Li YC (2007) *Solid State Commun* 142:114
38. Yu SQ, Chen SG, Zhang WW, Yu LH, Yin YS (2007) *Chem Phys Lett* 446:217
39. Doversat M, Karlsson L, Lindgren B, Sassenberg U (1998) *J Phys B* 31:795
40. Zhao WJ, Lei XL, Yan YL, Yang Z, Luo YH (2007) *Acta Phys Sinica* 56:5210
41. Wang CC, Zhao RN, Han JG (2006) *J Chem Phys* 124:194301
42. Koretsky GM, Knickelbein MB (1998) *Eur Phys J D* 2:273
43. Cao XY, Dolg M (2002) *Theor Chem Acc* 108:143
44. Cao XY, Dolg M (2003) *Mol Phys* 101:1967
45. Shen X, Fang L, Chen X, Lombardi JR (2000) *J Chem Phys* 113:2233
46. Alonso JA (2005) Bimetallic Clusters, Structure and Properties of Atomic Nanoclusters. Imperial College Press, London
47. Reddy BV, Khanna SN, Deevi SC (2001) *Chem Phys Lett* 333:465
48. Ouyang Y, Chen H, Zhong X (2006) *Theor Chem Acc* 115:32
49. Yin YS, Yu SQ, Zhang WW, Ye HN (2009) *J Mol Struct THEOCHEM* 902:1
50. Zhao WJ, Wang QL, Ren FZ, Luo YH (2007) *Acta Physica Sinica* 56:5746
51. Frisch MJ et al (2003) Gaussian 03, Gaussian. Inc., Pittsburgh, PA
52. Fu Z, Lemire GW, Bishea GA, Morse MD (1990) *J Chem Phys* 93:8420
53. Cai MF, Dzugan TP, Bondybey VE (1989) *Chem Phys Lett* 155:430
54. Moskovits M, Dilella DP, Lim W (1984) *J Chem Phys* 80:626
55. Purdum H, Montano PA, Shenoy GK, Morrison T (1982) *Phys Rev B* 25:4412
56. Leopold DG, Lineberger WC (1986) *J Chem Phys* 85:51
57. Arrington CA, Blume T, Morse MD, Doversat M, Sassenberg U (1994) *J Phys Chem* 98:1398
58. Becke AD (1993) *J Chem Phys* 98:5648
59. Lee C, Yang W, Parr RG (1988) *Phys. Rev. B* 37:785
60. Miehlich B, Savin A, Stoll H, Preuss H (1989) *Chem Phys Lett* 157:200
61. Hay PJ, Wadt WR (1985) *J Chem Phys* 82:284
62. Huelsen M, Weigand A, Dolg M (2009) *Theor Chem Acc* 122:23
63. [http://www.theochem.uni-stuttgart.de/pseudopotentials/clickpse\\_en.html](http://www.theochem.uni-stuttgart.de/pseudopotentials/clickpse_en.html)
64. Ouyang YF, Wang JC, Hou YH, Zhong XP, Du Y, Feng YP (2008) *J Chem Phys* 128:074305